Open Journal of Yangtze Gas and Oil, 2021, 6, 36-49
https://www.scirp.org/journal/ojogas
ISSN Online: 2473-1900
ISSN Print: 2473-1889

Adsorptive Removal of Pyridine from Aqueous Solution Using Natural Shale

Yi Wu[1,2], Kangle Ding[1,2*], Mei Zou[1,2], Zhenzhen Yu[1,2], Chao Han[1,2], Yan Liu[3], Fujia Guan[4]

[1]Key Laboratory of Exploration Technologies for Oil and Gas Resources, Ministry of Education, Yangtze University, Wuhan Campus, Wuhan, China
[2]College of Chemistry and Environmental Engineering, Yangtze University, Jingzhou, China
[3]College of Resources and Environment, Yangtze University, Wuhan Campus, Wuhan, China
[4]College of Petroleum Engineering, Yangtze University, Wuhan Campus, Wuhan, China
Email: *dingkl@yangtzeu.edu.cn

How to cite this paper: Wu, Y., Ding, K.L., Zou, M., Yu, Z.Z., Han, C., Liu, Y. and Guan, F.J. (2021) Adsorptive Removal of Pyridine from Aqueous Solution Using Natural Shale. *Open Journal of Yangtze Gas and Oil*, **6**, 36-49.
https://doi.org/10.4236/ojogas.2021.62004

Received: March 5, 2021
Accepted: April 19, 2021
Published: April 22, 2021

Abstract

The discharge of pyridine bearing wastewater into water bodies without a prior satisfactory treatment would pose significant public health risk as well as serious threat to the aquatic ecosystems. In this study, a natural shale from Yichang, China is investigated to determine its potential as a low-cost adsorbent for trace pyridine removal from wastewaters. The prepared shale samples without surface modification are characterized by Fourier transform infrared spectroscopy (FT-IR), X-ray diffraction (XRD) and scanning electron microscope (SEM). Kinetics and isotherms of pyridine from aqueous solutions onto shale are investigated on the basis of the experimental data. It is found that the shale samples with well-developed porosity are mainly composed of illite, quartz, calcite, chlorite and sericite. Several kinetic models (viz. pseudo-first-order, pseudo-second-order, two-constant rate, intra-particle diffusion and Elovich) as well as isotherm models (Langmuir, Freundlich and Temkin) are applied to test the experimental data for pyridine removal. The kinetics of the adsorption of pyridine by shale follows a pseudo-second-order rate law with the adsorption data being best described by the Freundlich isotherm model. The preliminary study shows that natural shale obtained from sedimentary basins may be used as a potential low-cost adsorbent for the removal of trace pyridine from effluents.

Keywords

Natural Shale, Sedimentary Basins, Pyridine, Adsorption, Kinetics, Isotherms

1. Introduction

Pyridine is a common N-heterocyclic aromatic compound in effluents discharged from chemical factories, coking plants, pharmaceutical factories and the related industries [1]. As one of the priority pollutants listed by the United States Environmental Protection Agency [2], pyridine exhibits significant toxicity toward organisms and potential mutagenicity, teratogenicity as well as carcinogenicity to human beings [1] [3]. Especially, in comparison with other aromatic hydrocarbons pyridine is more difficult to be degraded by indigenous microorganisms, leading to its long-term stable existence in the environment. The discharge of pyridine bearing wastewater into water bodies without a prior satisfactory treatment would pose significant public health risk as well as serious threat to the aquatic ecosystems. In wastewater, the typical concentration of pyridine and its associated compounds may vary in the range of 20 - 300 mg/L [2] [4] [5]. A variety of physic-chemical treatment techniques have been developed for the removal of pyridine from wastewater, such as photocatalysis, ion exchange, extraction, foam fractionation, gamma irradiation, microwave radiation, electrochemistry, oxidation, biological treatment and adsorption. Among all the mentioned techniques, adsorption is one of the simplest, effective and economical method for the removal of low concentrations of organic pollutants from large volumes of potable water, process effluents, wastewater, and aqueous solutions [6]. Over the last decade, activated carbon (AC) has been proved to be effective for the removal of pyridine and its derivatives from industrial effluents [7] [8]. However, the disadvantage associated with AC lies in, the need for a costly regeneration system, the generation of carbons fines due to the brittle nature of carbons as well as its high initial manufacture cost [9] [10]. These make AC less economically viable as an adsorbent and led many investigators to search low-cost, naturally occurring adsorbents to remove trace pyridines from wastewater.

Yichang is located in central China, the southwest of Hubei Province, the upper and middle reaches of the Yangtze River. The shale in Yichang is a fine-grained sedimentary rock, generally characterized by large specific surface area and high porosity. Most previous studies are conducted with a focus on methane adsorption behavior on shale matrix [11]. To the best of our knowledge, there is no data available in literature about the removal of pyridines by shale. The objectives of this study are to:

1) Examine the feasibility of raw shale for pyridine removal from wastewater without any pretreatment procedures;

2) Study the adsorption characteristics, *i.e.* kinetics and isotherms of pyridine from aqueous solutions onto shale.

2. Materials and Methods

2.1. Materials and Preparation of Adsorbents

Pyridine, hydrochloric acid, sodium hydroxide and other chemicals are analytical reagents and purchased from Aladdin Industrial Corporation (Shanghai, China). Natural shale in this study is obtained from Yiye-1 shale gas well in Yichang, Hubei province of China at the burial depth of 1835.0 m. The shale sample is crushed with a mechanical rock crusher, ground in a ceramic mill, and then sieved to the desired particle size fractions. The sample of the particle size 177 μm is washed using magnetic stirrer with the distilled water to remove any dissolved salts. After filtration, the washed sample is dried at 110˚C overnight in an electric oven (Tianjin Taisite Instrument Co., Ltd., 101-1AB). The dry shale sample is kept in a desiccator over silica gel desiccant until use in characterization and adsorption experiments.

2.2. Instruments

The X-ray diffraction (XRD) technique is used to obtain the semi-qualitative mineralogical compositions of the shale samples. The samples are mechanically crushed and ground to size of <200 mesh. XRD data are collected at room temperature with a PANalytical X'Pert PRO X-ray diffractometer (PANalytical Co., Almelo, Netherlands). About 30 mg of powdered solid samples are kept in a quartz block and pressed onto the quartz block using a glass slide to obtain a uniform distribution. The 2θ Bragg angles are scanned over a range of 5 - 85 at a scanning speed of 6.25/min, using graphite monochromated Cu-K_α radiation source and a nickel filter. The tube current and the tube voltage is 30 mA and 40 kV, respectively. The experiment parameters are as followed: DS = 1/4, SS = 1/8, RS = 5.0 mm. The computer automates the data collection and data reduction steps of the analysis. To obtain a semiquantitative measurement of the mineral components of a given sample, the maximum intensity of each identified mineral is measured and compared to the standard intensity obtained from a pure mineral sample.

The FT-IR spectra are obtained in a diffuse reflectance infrared Fourier transform spectroscopy (DRIFTS) mode using the micro sampling cup of a Spectra-Tech diffuse reflectance accessory against a KBr background on a Nicolet 750 FT-IR spectrometer (Thermo Nicolet Corporation, Waltham, MA, DTGS detector; Nichrome source; KBr beam splitter). A small amount of the shale samples is finely ground, mixed with dried potassium bromide (Merck, Sharp and Dhome Ltd., Shanghai, China, spectroscopic grade) in the ratio of 1:100, and pressed into pellets for a spectrum test. The FT-IR spectra are collected and manipulated using the Thermo Electron software, OMNIC 7.0, supplied from the manufacturer of the spectrometer by averaging 32 scans at a spectral resolution of 4 cm^{-1} under a dried nitrogen flow (10 cm^3/min) condition. All spectra are smoothed using the "automatic smooth" function of the above software, which uses the Savitsky-Golay algorithm (95-point moving second-degree polynomial). After that, the baseline is corrected using the "automatic baseline correct" and the spectra scale is normalized with the "normalize scale" function. The spectroscopic region from 4,000 cm^{-1} to 400 cm^{-1} is used for the hierarchical cluster analysis.

Morphology of the shale samples is observed by a field emission-scanning electron microscope (FE-SEM, Model MIRA3 -XMU, TESCAN Czech Republic) operated at an acceleration voltage of 15 kV. The samples are observed under the conditions of 10.0 k and 50.0 k magnifications.

2.3. Adsorption Procedure

In batch adsorption experiments, accurately weighed shale samples (0.1 - 1.5 g) and 30 mL of the aqueous solution containing different initial concentrations of pyridine (2.0 - 50 mg/L) are put into a glass-stoppered flask. The flask is darkly brown-colored to prevent photoxidation. The pH of the solution is adjusted with HCl or NaOH solution by using a pH meter (Model PB-10, Shanghai Cany Precision Instrument Co., Ltd, China). The flask is subsequently capped with the glass stopper and shaken in a temperature-controlled water bath shaker (Model SHA-B, Tianjin Saidlis Experimental Analytical Instrument Factory, China) for 2 h at the temperature range of 25˚C - 45˚C. At preset contact times, the concentrations of pyridine in the solution are analyzed for residual concentration of pyridine at λ_{max} = 256 nm [7] using a 722N UV-vis spectrophotometer (Shanghai AuCy Scientific Instrument Co., Ltd., China). The amount adsorbed is calculated from the concentration of the pyridine solution before and after the adsorption experiments using a Beer's law plot to interpolate concentrations. Pyridine uptake at equilibrium, q_e (mg/g), is calculated by the equation, $q_e = (C_0 - C_e) V/W$. The C_0 and C_e (mg/L) are the concentrations of pyridine at initial and at equilibrium, respectively. V is the volume of the solution (L) and W is the mass of dry adsorbent used (g). The calibration curves between absorbance and the concentration of the pyridine solution are established. The calibration plot of absorbance versus concentration of pyridine shows a linear variation. The standard curve is given as $y = 31.895x + 0.002$, $R^2 = 0.9994$, where y is the absorbance and x is the pyridine concentration.

3. Results and Discussion

3.1. Characterization of Adsorbents

The FT-IR spectra of the shale sample are given in **Figure 1**. The broad and strong band in the range of 3140 - 3620 cm^{-1} is assigned to the –OH stretching vibration in hydroxyl groups of constitution water and interlayer water of clay minerals [12]. The peak at 1410 cm^{-1} is attributed to the stretching vibration of C-O in the carbonate anion (CO_3^{2-}) of calcite [13]. The intense band in the range of 1000 - 1100 cm^{-1} is ascribed to the Si-O vibration in quartz [14]. The peaks at 515 - 795 cm^{-1} indicate the vibration of Si-O, Al-O-H and Si-O-Al [14].

X-ray diffraction patterns of the shale sample are exhibited in **Figure 2**. Quantitative mineralogical analyses by XRD (**Figure 2**) reveal that the typical shale sample primarily consists of illite (45.94 wt%), quartz (38.05 wt%), calcite (11.28 wt%), chlorite (3.04 wt%) and sericite (1.68 wt%).

The SEM micrograph in **Figure 3** is employed to evaluate the morphological structure of the shale. **Figure 3** shows that the prepared the shale sample is characterized by various visible fractures and pore structures with different diameters, which may be derived from naturally and/or artificially occurring disintegration of the shale matrix. The well-developed porosity of the shale may favor pyridine removal during the actual effluent treatment process.

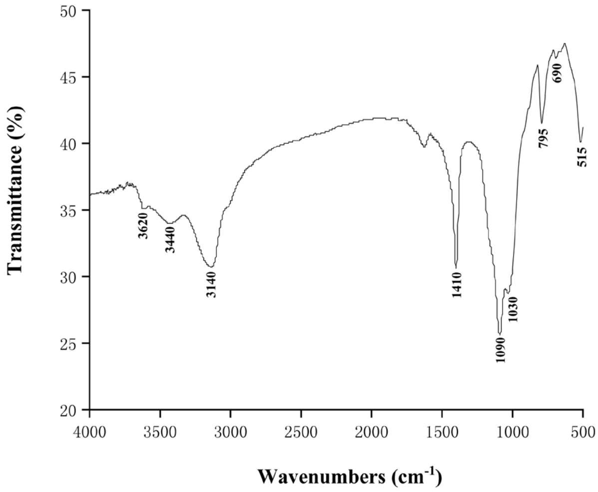

Figure 1. FT-IR spectra of the shale sample.

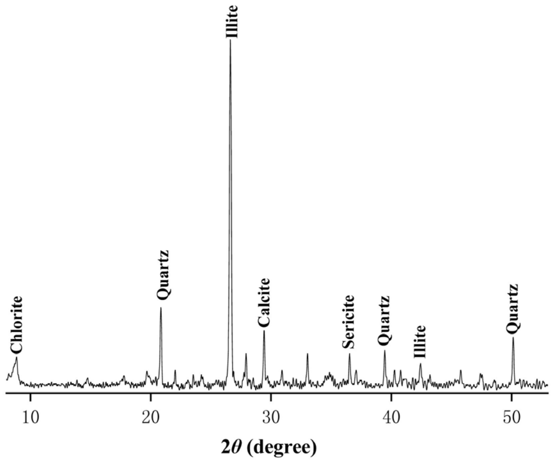

Figure 2. X-ray diffraction patterns of the shale sample.

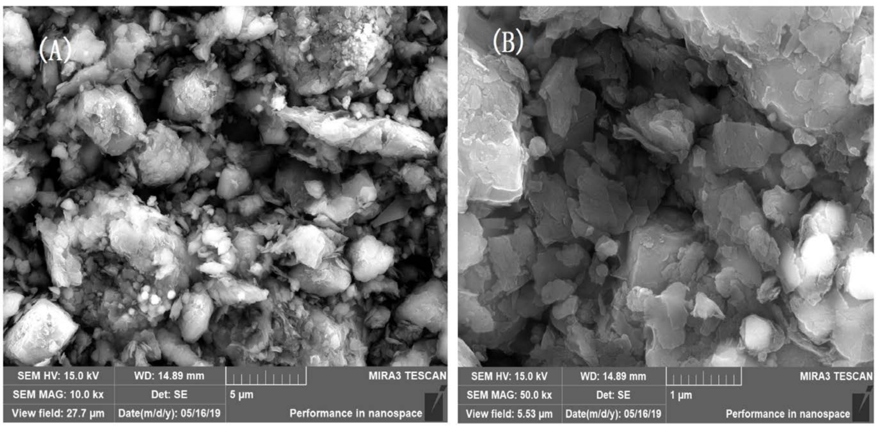

Figure 3. The SEM images of the shale sample at different magnifications.

3.2. Adsorption Kinetics

The study of adsorption kinetics can provide valuable insights into the uptake rate of sorbents, the adsorption mechanisms as well as the proper design and model for the adsorption process. The experimental kinetic data of adsorption of pyridines onto the shale are analyzed by pseudo-first order, pseudo-second order, Elovich equation, intra-particle diffusion and two-constant rate equation [14], respectively. The fitting results are listed in **Table 1**. The pseudo first order model is the earliest developed equation that explains reversible equilibrium between adsorbate and adsorbent, assuming the rate in which the sites becoming occupied is exactly equal to number of vacant sites [14]. The pseudo-first-order rate equation is generally described by the following equation:

Table 1. Kinetic parameters of adsorption of pyridine on shale.

Kinetic model	Parameters	298 K	R^2
Pseudo-first-order	q_e (mg·g^{-1}) k_1 (min^{-1})	0.516 0.0169	0.891
Pseudo-second-order	q_e (mg·g^{-1}) k_2 (g·mg^{-1}·min^{-1})	0.530 0.186	0.999
Two-constant	a (mg·g^{-1}·min^{-1}) b [(mg·g^{-1})$^{-1}$]	0.309 0.0904	0.970
Intra-particle diffusion	I (mg·g^{-1}) K_{id} (mg·g^{-1}·min$^{-0.5}$)	0.3831 0.00794	0.899
Elovich	α (mg·g^{-1}·min^{-1}) β (g·mg^{-1})	33.239 23.981	0.974

$$\ln\left(q_e - q_t\right) = \ln q_e - k_1 t \tag{1}$$

where q_e and q_t are the amounts of pyridine adsorbed (mg/g) at equilibrium and at time t (min), respectively. k_1 is the rate constant of adsorption (min^{-1}) and calculated from the plots of ln(q_e − q_t) versus t for different concentrations of pyridine. The results of k_1 and correlation coefficients (R^2) are shown in **Table 1**.

Pseudo-second-order kinetic model is based on the assumption that the rate-determining step may be a chemical sorption involving valence forces through sharing or exchange of electrons between adsorbent and adsorbate. The pseudo-second-order kinetic model is expressed as follows:

$$\frac{t}{q_t} = \frac{1}{k_2 q_e^2} + \frac{t}{q_e} \tag{2}$$

where k_2 is the pseudo-second-order rate constant (g·mg^{-1}·min^{-1}). Values of k_2 and q_e are calculated from the intercept and slope of the plots of t/q versus t. The results of k_2 and correlation coefficients (R^2) are shown in **Table 1**.

The Elovich equation is often used to interpret the kinetics of sorption and successfully describe the predominantly chemical sorption on highly heterogeneous sorbents. It is based on kinetic principle assuming that the sorption sites increase exponentially with sorption, which implies a multilayer sorption and each layer exhibits a different activation energy for chemisorption. The Elovich equation can be written, in its integrated form, as follows:

$$q_t = \frac{1}{\beta}\ln(\alpha\beta) + \frac{1}{\beta}\ln t \quad (3)$$

where, α is the initial adsorption rate ($mg \cdot g^{-1} \cdot min^{-1}$) and β is the desorption constant ($g \cdot mg^{-1}$). The term $1/\beta$ indicates the number of sites available for adsorption. A plot between q_t versus $\ln(t)$ yields a linear relationship with a slope of $(1/\beta)$ and an intercept of $(1/\beta)\ln(\alpha\beta)$. The values of α, β and correlation coefficients are shown in **Table 1**.

The intra-particle diffusion model is used to identify the diffusion mechanism. This kinetic model considers the rate limiting step of transport of adsorbates from bulk into adsorbents and is expressed as follows:

$$q_t = I + K_{id}\sqrt{t} \quad (4)$$

where k_{id} is the intra-particle diffusion rate constant ($mg \cdot g^{-1} \cdot min^{-0.5}$) and I is the intercept of vertical axis ($mg \cdot g^{-1}$). According to Equation (4), a plot of q_t versus $t_{1/2}$ should be a straight line with a slope k_{id} and intercept I when adsorption mechanism follows the intra-particle diffusion process. The values of k_{id} and correlation coefficients are listed in **Table 1**.

The two-constant model is a useful empirical equation. With two fitting parameters this model is quite flexible to predict the extraction kinetics, but note that this equation has not been rigorously derived or explained. The two-constant kinetic model is expressed as follows:

$$\ln q_t = \ln a + b\ln t \quad (5)$$

where a is the initial desorption rate constant ($mg \cdot g^{-1} \cdot min^{-1}$) and b is the desorption rate coefficient [$(mg \cdot g^{-1})^{-1}$]. The values of a and b and correlation coefficients are listed in **Table 1**. The fitting curves and calculated parameters of the four adsorption kinetics models at different temperatures are shown in **Figure 4** and **Table 1**, respectively.

Since each fitting equation has different assumptions, the correlation coefficient (R^2) represents the correlation between the equation and the adsorption curves. It is generally believed that when the correlation coefficient R^2 of the fitting equation reaches ≥ 0.99, the adsorption curves conform to the fitting equation and the adsorption process satisfies the assumption of the fitting equation. Fitting the adsorption curve can also contribute to the prediction of adsorption equilibrium and adsorption capacity. The correlation coefficients of the pseudo-first-order model, two-constant model, intra-particle diffusion model and Elovich kinetic model are found to be less than 0.99. Furthermore, the adsorption capacities calculated using these fitting models greatly deviate from the experiment data. By contrast, the correlation coefficients of the pseudo-second-order kinetic model are more than 0.99, suggesting that the adsorption of pyridine on shale matches well with the pseudo-second-order kinetic model. Our kinetic results for the adsorption of pyridine by shale are consistent with some previous studies using bamboo charcoal [15], mesoporous silica [16] and polymeric adsorbents [3] [17] [18].

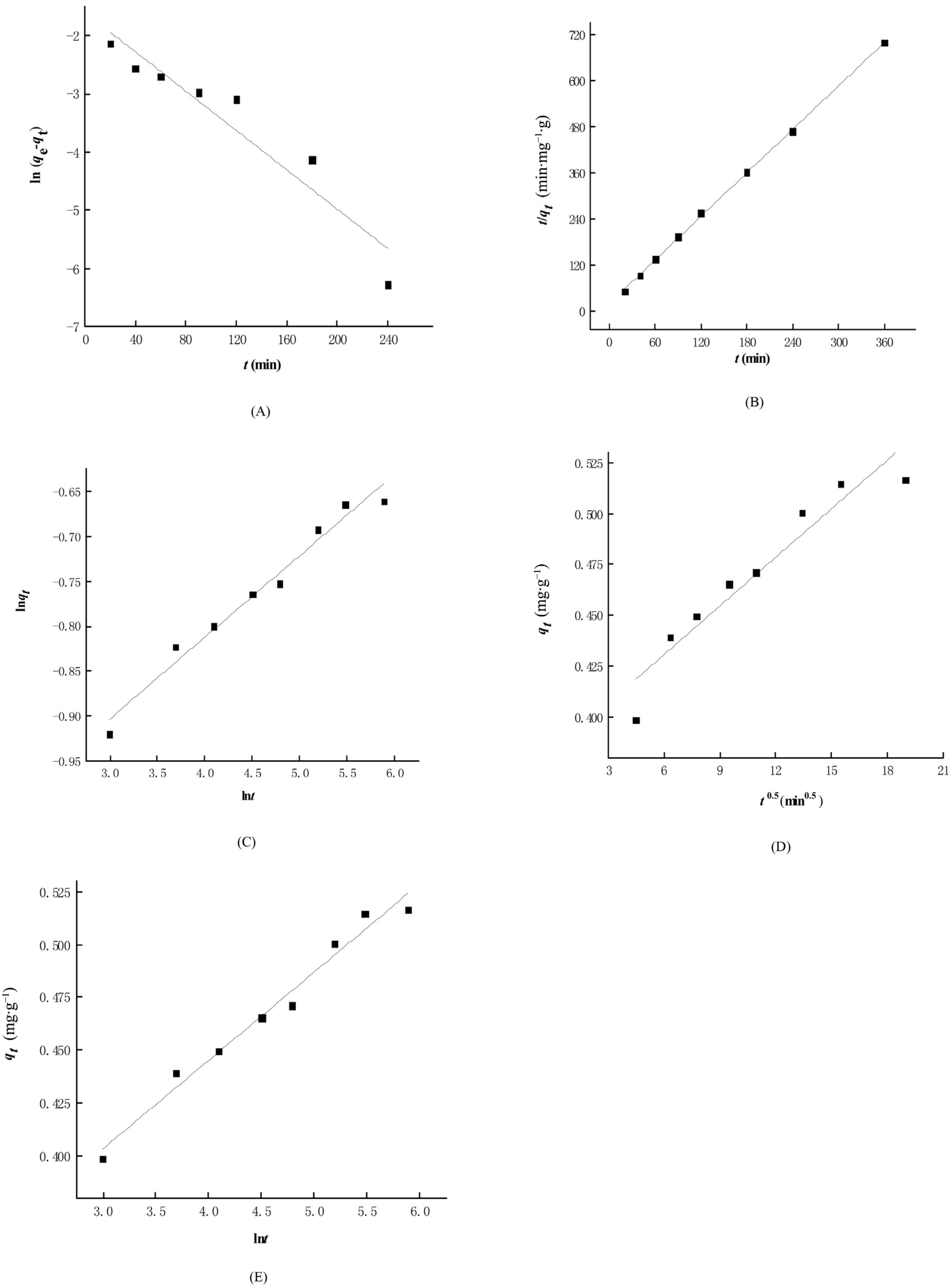

Figure 4. Various adsorption kinetics model fitting curves for the removal of pyridine by shale: (A) Pseudo-first-order model; (B) Pseudo-second-order model; (C) Two-constant model; (D) Intra-particle diffusion model; (E) Elovich model.

3.3. Adsorption Isotherms

Some isotherm models are presented to describe the adsorption process such as Langmuir, Freundlich, Tempkin, and Redlich-Peterson. A survey of adsorption isotherms by Awad *et al.* (2019) reveals that Langmuir, Freundlich and Temkin are more frequently employed by previous researchers to investigate the simulation experiments. Based on the statistical result of Awad *et al.* (2019), we tentatively examine the present experimental data using Equations (6), (7) and (8) as followed.

Langmuir equation:

$$\frac{C_e}{q_e} = \frac{C_e}{q_{max}} + \frac{1}{K_L \times q_{max}} \tag{6}$$

Freundlich equation:

$$\lg q_e = \frac{\lg C_e}{n} + \lg K_F \tag{7}$$

Tempkin isotherm is represented by the following equation:

$$q_e = \frac{RT}{b_T} \ln K_T + \frac{RT}{b_T} \ln C_e \tag{8}$$

where C_e stands for equilibrium concentration of pyridines (mg/L), q_e denotes the equilibrium adsorption capacity (mg/g), q_{max} refers to maximum adsorption capacity (mg/g), K_L designates Langmuir constant (L/mg), K_F represents the Freundlich constant (mg/g)(mg/L)$^{(-1/n)}$, K_T signifies the equilibrium binding constant corresponding to the maximum binding energy, and b_T is equilibrium Temkin binding constant, related to the heat of adsorption. The fitting curves of the Langmuir, Freundlich and Temkin isotherms were exhibited in **Figure 5**.

The related model parameters and the corresponding regression coefficients are listed in **Table 2**. The Freundlich model with the highest R^2 values (**Table 2**) demonstrates its best describing the whole process for pyridine removal in comparison with the Langmuir and Temkin models.

Table 2. Parameters of adsorption isotherm models.

Model	Parameters	298 K	R^2
Langmuir	K_L (L/mg)	0.003	0.984
	q_{max} (mg/g)	3.508	
Freundlich	K_F (mg/g)(mg/L)$^{(-1/n)}$	0.008	0.994
	n	1.103	
Temkin	K_T	0.047	0.856
	b_T	2.049	

3.4. Comparison with Other Studies Using Natural and/or Synthetic Materials

It should be noted that some previous researchers have carried out laboratory experiments to examine the performance of natural and/or synthetic materials as adsorbents for pyridine removal (**Table 3**). From **Table 3** it could be concluded that the Langmuir and Freundlich models are regularly utilized to test the isothermal experimental data.

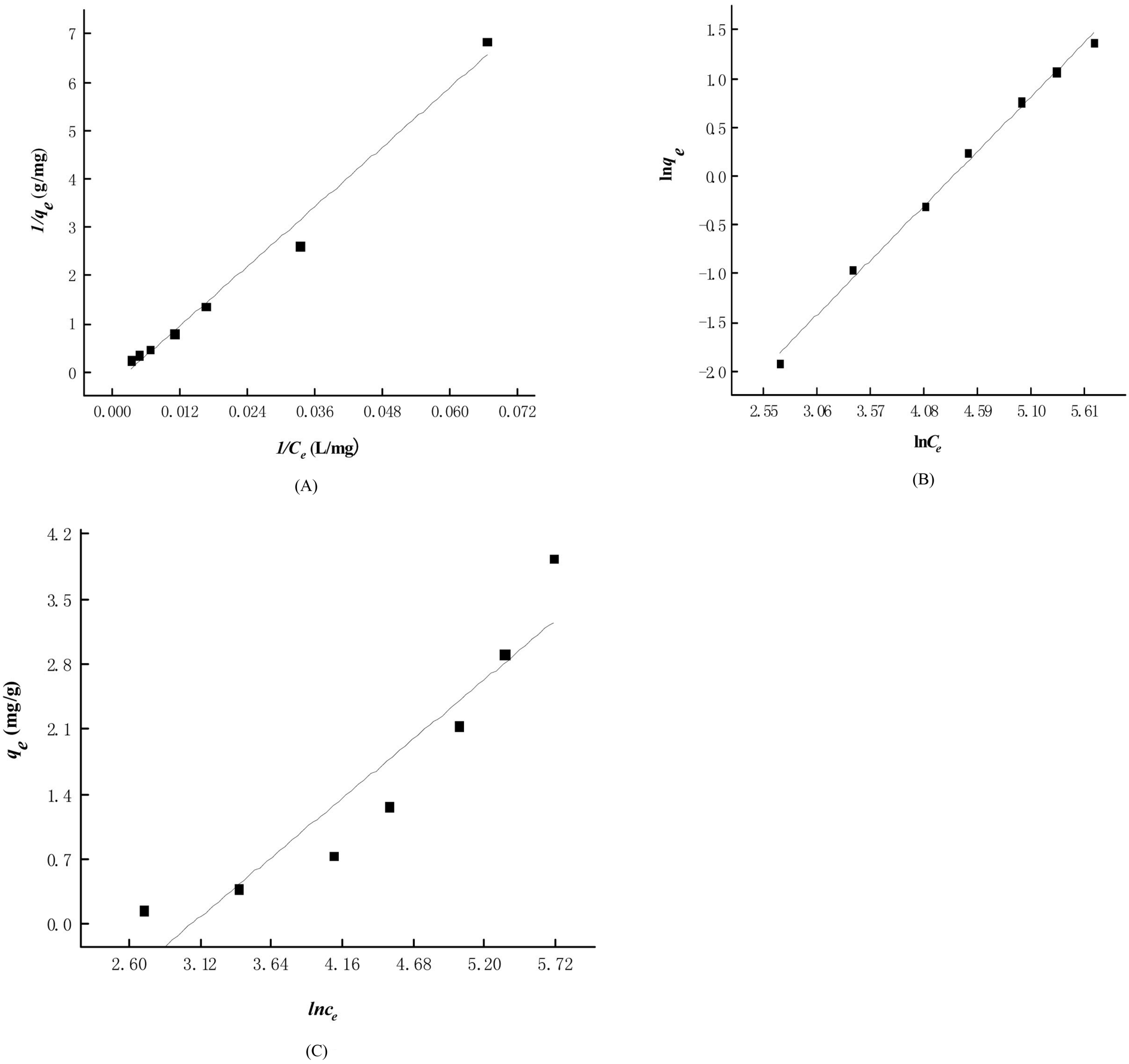

Figure 5. Adsorption isotherms of pyridine on shale: (A) Langmuir model; (B) Freundlich model; (C) Temkin model.

Our investigation reveals that the removal of pyridine by shale from aqueous solution is much better demonstrated by the Freundlich adsorption isotherm model than the Langmuir model. This result coincides with former studies employing minerals widespread in sedimentary basins including natural apatite [24], kaolinite [25], and montmorillonite [25]. Our preliminary study shows that natural shale exhibits a limited adsorption capacity (of an order of magnitude of 1 mg/g) in **Table 2**. Nevertheless, unmodified shale may be potentially applied to treat wastewaters containing trace pyridines. Should the adsorption capacity of the natural shale be further improved by different modifications in the next wok, natural shale is undoubtedly one of the promising candidates for pyridine bearing effluents treatment since it is environment-friendly, cost-effectively and rich in nature.

Table 3. Isothermal models for removal of pyridine by natural and/or synthetic adsorbents.

Adsorbents	Isotherm models	References
α-Al_2O_3	Langmuir, FFG	[19]
Apatite	Freundlich	[20]
Activated carbon	Langmuir	[7]
Activated carbon	Toth and Radke-Prausnitz	[4]
Activated carbon fibers	Langmuir	[8]
Activated carbon cloth	Prausnitz-Radke	[21]
Bagasse fly ash	Langmuir	[2]
Bamboo charcoal	Freundlich	[16]
Carbon nanotube	Freundlich	[22]
Ion-exchange resin	Langmuir, Freundlich	[23]
Iron powder	Langmuir, FFG	[19]
Kaolinite	Freundlich	[24]
Mesoporous silica	Langmuir	[17]
Montmorillonite	Freundlich	[24]
Poly 4-vinyl aniline-co-DVB	Freundlich	[25]
Polymeric adsorbents	Langmuir, Freundlich	[3]
Post-crosslinked fiber	Freundlich	[18]
Rice husk ash	Redlich-Peterson	[4]
Spent oil shale	Langmuir	[26]
Zeolite	Langmuir-Freundlich	[27]
Shale	Freundlich	This study

4. Conclusion

Preliminary laboratory experiments are carried out to investigate the performance of natural shale from Yichang, China as an adsorbent for pyridine removal from wastewaters. It is found that the prepared shale samples with well-developed porosity are mainly composed of illite, quartz, calcite, chlorite and sericite. The kinetics of the adsorption processes conforms to a pseudo-second-order rate law with the adsorption data characterized by the Freundlich isotherm model. The preliminary results denote that natural shale collected from sedimentary basins may be employed as one of the potential low-cost adsorbents for treating effluents containing trace pyridine. Modification methods of shale still need further investigation in the next work.

Acknowledgements

We gratefully acknowledge financial support by the National Natural Science Foundation of China (No. 41730424; 41472095) and the Open Fund of Key Laboratory of Exploration Technologies for Oil and Gas Resources (Yangtze University), Ministry of Education (No. K2018-05).

Conflicts of Interest

The authors declare no conflicts of interest regarding the publication of this paper.

References

[1] Padoley, K.V., Mudliar, S.N. and Pandey, R.A. (2008) Heterocyclic Nitrogenous Pollutants in the Environment and Their Treatment Options—An Overview. *Bioresource Technology*, **99**, 4029-4043. https://doi.org/10.1016/j.biortech.2007.01.047

[2] Lataye, D.H., Mishra, I.M. and Mall, I.D. (2006) Removal of Pyridine from Aqueous Solution by Adsorption on Bagasse Fly Ash. *Industrial and Engineering Chemistry Research*, **45**, 3934-3943. https://doi.org/10.1021/ie051315w

[3] Zhu, Q., Moggridge, G.D. and Ainte, M. (2016) Adsorption of Pyridine from Aqueous Solutions by Polymeric Adsorbents MN 200 and MN 500. Part 1: Adsorption Performance and PFG-NMR Studies. *Chemical Engineering Journal*, **306**, 67-76. https://doi.org/10.1016/j.cej.2016.07.039

[4] Lataye, D.H., Mishra, I.M. and Mall, I.D. (2008) Pyridine Sorption from Aqueous Solution by Rice Husk Ash (RHA) and Granular Activated Carbon (GAC): Parametric, Kinetic, Equilibrium and Thermodynamic Aspects. *Journal of Hazardous Materials*, **154**, 858-870. https://doi.org/10.1016/j.jhazmat.2007.10.111

[5] Subbaramaiah, V., Srivastava, V.C. and Mall, I.D. (2013) Catalytic Wet Peroxidation of Pyridine Bearing Wastewater by Cerium Supported SBA-15. *Journal of Hazardous Materials*, **248**, 355-363. https://doi.org/10.1016/j.jhazmat.2013.01.018

[6] Singh, N.B., Nagpal, G. and Agrawal, S. (2018) Water Purification by Using Adsorbents: A Review. *Environmental Technology and Innovation*, **11**, 187-240. https://doi.org/10.1016/j.eti.2018.05.006

[7] Mohan, D., Singh, K.P., Sinha, S. and Gosh, D. (2004) Removal of Pyridine from Aqueous Solution Using Low Cost Activated Carbons Derived from Agricultural Waste Materials. *Carbon*, **42**, 2409-2421. https://doi.org/10.1016/j.carbon.2004.04.026

[8] Li, B., Lei, Z., Zhang, X. and Huang, Z. (2010) Adsorption of Simple Aromatics from Aqueous Solutions on Modified Activated Carbon Fibers. *Catalysis Today*, **158**, 515-520. https://doi.org/10.1016/j.cattod.2010.08.014

[9] Ahmaruzzaman, M. (2008) Adsorption of Phenolic Compounds on Low-Cost Adsorbents: A Review. *Advances in Colloid and Interface Science*, **143**, 48-67. https://doi.org/10.1016/j.cis.2008.07.002

[10] Lin, S.H. and Juang, R.S. (2009) Adsorption of Phenol and Its Derivatives from Water Using Synthetic Resins and Low-Cost Natural Adsorbents: A Review. *Journal of Environmental Management*, **90**, 1336-1349. https://doi.org/10.1016/j.jenvman.2008.09.003

[11] Tang, X., Ripepi, N., Rigby, S., Mokaya, R. and Gilliland, E. (2019) New Perspectives on Supercritical Methane Adsorption in Shales and Associated Thermodynamics. *Journal of Industrial and Engineering Chemistry*, **78**, 186-197. https://doi.org/10.1016/j.jiec.2019.06.015

[12] Rouxhet, P.G., Samudacheata, N., Jacobs, H. and Anton, O. (1977) Attribution of the OH Stretching Bands of Kaolinite. *Clay Minerals*, **12**, 171-179. https://doi.org/10.1180/claymin.1977.012.02.07

[13] Ding, K., Li, S., Yue, C. and Zhong, N. (2007) Simulation Experiments on Thermochemical Sulfate Reduction Using Natural Gas. *Journal of Fuel Chemistry and Technology*, **35**, 401-406. https://doi.org/10.1016/S1872-5813(07)60025-5

[14] Więckowski, T. and Wiewióra, A. (1976) New Approach to the Problem of the Interlayer Bonding in Kaolinite. *Clays and Clay Minerals*, **24**, 219-223. https://doi.org/10.1346/CCMN.1976.0240502

[15] Awad, A.M., Shaikh, S.M.R., Jalab, R., Gulied, M.H., Nasser, M.S., Benamor, A. and Adham, S. (2019) Adsorption of Organic Pollutants by Natural and Modified Clays: A Comprehensive Review. *Separation and Purification Technology*, **228**, Article ID: 115719. https://doi.org/10.1016/j.seppur.2019.115719

[16] Liao, P., Yuan, S., Xie, W., Zhang, W., Tong, M. and Wang, K. (2013) Adsorption of Nitrogen-Heterocyclic Compounds on Bamboo Charcoal: Kinetics, Thermodynamics, and Microwave Regeneration. *Journal of Colloid and Interface Science*, **390**, 189-195. https://doi.org/10.1016/j.jcis.2012.09.037

[17] Singh, K., Chandra, B., Rhyman, L. and Ramasami, P. (2016) Effective Adsorption of Pyridine (Py)—Onto Mesoporous Silica Derived from De-Oiled Mustard Cake (DOMC): Experimental and Theoretical Study. *Journal of Environmental Chemical Engineering*, **4**, 1383-1392. https://doi.org/10.1016/j.jece.2016.01.033

[18] Zhang, Y. and Li, D. (2010) Adsorption of Pyridine on Post-Crosslinked Fiber. *Journal of Scientific and Industrial Research*, **69**, 73-76.

[19] Ardizzone, S., Høiland, H., Lagioni, C. and Sivieri, E. (1998) Pyridine and Aniline Adsorption from an Apolar Solvent: The Role of the Solid Adsorbent. *Journal of Electroanalytical Chemistry*, **447**, 17-23. https://doi.org/10.1016/S0022-0728(98)00007-2

[20] Bouyarmanea, H., Ei Asria, S., Ramib, A., Rouxc, C., Mahlyb, M.A., Saoiabia, A., Coradinc, T. and Laghzizila, A. (2010) Pyridine and Phenol Removal Using Natural and Synthetic Apatites as Low Cost Sorbents. Influence of Porosity and Surface Interactions. *Journal of Hazardous Materials*, **181**, 736-741. https://doi.org/10.1016/j.jhazmat.2010.05.074

[21] Alonso-Davila, P., Torres-Rivera, O.L., Leyva-Ramos, R. and Ocampo-Perez, R. (2012) Removal of Pyridine from Aqueous Solution by Adsorption on an Activated Carbon Cloth. *Clean-Soil Air Water*, **40**, 45-53. https://doi.org/10.1002/clen.201100049

[22] Zhao, B., Liang, H., Han, D., Qiu, D. and Chen, S. (2007) Adsorption of Pyridine from Aqueous Solution by Surface Treated Carbon Nanotubes. *Separation Science and Technology*, **42**, 3419-3427. https://doi.org/10.1080/01496390701511689

[23] Akita, S. and Takeuchi, H. (1993) Sorption Equilibria of Pyridine Derivatives in Aqueous Solution on Porous Resins and Ion Exchange Resins. *Journal of Chemical Engineering of Japan*, **26**, 237-241. https://doi.org/10.1252/jcej.26.237

[24] Baker, R.A. and Luh, M.D. (1971) Pyridine Sorption from Aqueous Solution by Montmorillonite and Kaolinite. *Water Research*, **5**, 839-848. https://doi.org/10.1016/0043-1354(71)90020-0

[25] Mathidala, S. and Ogunlaja, A.S. (2019) Selective Removal of Pyridine in Fuel by Imprinted Polymer (Poly 4-vinyl aniline-co-DVB) as Adsorbent. *Petroleum Science and Technology*, **37**, 1691-1703. https://doi.org/10.1080/10916466.2019.1602641

[26] Zhu, S., Bell, P.R.F. and Greenfield, P.F. (1988) Isotherm Studies on Sorption of Pyridine and Quinoline onto Rundle Spent Shale. *Fuel*, **67**, 1316-1320. https://doi.org/10.1016/0016-2361(88)90110-X

[27] Bludau, H., Karge, H.G. and Niessen, W. (1998) Sorption, Sorption Kinetics and Diffusion of Pyridine in Zeolites. *Microporous and Mesoporous Materials*, **22**, 297-308. https://doi.org/10.1016/S1387-1811(98)00093-6